

Atomic Energy of Canada Limited

PRIMARY COOLANT pH FOR CONTROL OF CANDU PLANT AGING

by

K.A.Burrill, E.L.Cheluget, D.G.Miller, and C.W.Turner*

Reactor Chemistry Branch
*Heat Exchanger Technology Branch
Chalk River Laboratories
Chalk River, Ontario

1998 September

Paper submitted to CNS Conference, Toronto, Ontario, 1998 October 18-21.

Atomic Energy of Canada Limited

PRIMARY COOLANT pH FOR CONTROL OF CANDU PLANT AGING

by

K.A.Burrill, E.L.Cheluget, D.G.Miller, and C.W.Turner*

ABSTRACT

Plant aging can be defined as any degradation with time of system performance which increases the operator's difficulty in maintaining operation within design specification. Degradation can be a physical change in a component beyond the design value, e.g. surface roughness, or a change in operating conditions, e.g. RIHT rise. This paper focuses on the corrosion of the carbon steel piping in the CANDU primary circuit and the aging issues that arise. In one approach, a small reduction in the coolant pH has been recommended to operating plants which will slow those aging issues driven by dissolved iron transport around the primary circuit. In addition, chemical decontamination of the entire HTS is suggested to restore primary circuit surfaces to near-original conditions.

Reactor Chemistry Branch
*Heat Exchanger Technology Branch
Chalk River Laboratories
Chalk River, Ontario

1998 September

PRIMARY COOLANT pH FOR CONTROL OF CANDU PLANT AGING

by

K.A.Burrill, E.L.Cheluget, D.G.Miller, and C.W.Turner*

1. INTRODUCTION

The slow corrosion of plant piping and the transport of corrosion products by the heat transport fluid will alter system performance. Deposition of corrosion products in the tubes in the steam generators can produce magnetite deposits which increase the hydraulic surface roughness of the boiler tubes and reduce the flow rate through the boiler. The importance of coolant pH in controlling corrosion and corrosion product transport in the CANDU heat transport system (HTS) is discussed here.

Figure 1 introduces the 'iron transport theory' for the HTS which may be used to predict the role of coolant pH in HTS aging caused by corrosion and corrosion product transport. The essence of the theory is the normal solubility behaviour of magnetite in the heavy water coolant over the pH and temperature range found in the HTS (Burrill, 1998). Coolant enters the reactor core slightly supersaturated in dissolved iron relative to the equilibrium solubility, illustrated with the curve for pH 10.3. The coolant leaves the core heated by about 50°C and is now highly unsaturated in dissolved iron since there is nominally no iron in the core. There is little change in the dissolved iron concentration along the stainless steel end-fitting. On reaching the carbon steel outlet feeder, the coolant turbulence at its high Reynolds number combine with the unsaturated coolant to produce flow accelerated corrosion (FAC) of the steel surface (Burrill, 1995). Dissolved iron is added to the coolant all along the outlet feeder pipe. On entering the steam generator, the water is cooled and the dissolved iron begins to deposit on the tubes as the magnetite solubility falls below the dissolved iron concentration at the local wall temperature. Such precipitation is expected in the U-bend and cold leg regions. Precipitation is still only 90% complete as the coolant enters the inlet feeder pipe, so magnetite continues to grow all along the inlet feeder pipe and along the inlet end-fitting. Precipitation stops at the core inlet region, where the water temperature begins to rise and the coolant once again becomes unsaturated in dissolved iron.

This theory supports the observed slow changes in operating conditions of the HTS with time that contribute to the aging process. The FAC of the outlet feeders adds the iron to the coolant. These feeder surfaces become hydraulically rough by scalloping which increases the pressure drop across them. Magnetite deposits in the steam generator tubes also increase the surface roughness and add to the pressure drop. As well, the deposits contain radioactive corrosion products which causes gamma radiation fields to rise slowly. The deposits also add to the heat transfer resistance across the tubes and result in a rise in the coolant temperature (T) at the reactor inlet header (RIH). Deposits on the inlet piping surfaces increase their hydraulic surface roughness, further adding to the pressure drop around the HTS. Finally, it is postulated that these magnetite deposits are slowly eroded as they grow and introduce particulate corrosion products to the coolant. These particles deposit on all HTS surfaces. Those deposited in the reactor core become radioactive, e.g. cobalt impurity will give Co-60. The particles dissolve as they are irradiated and the dissolved radioactive impurities are subsequently incorporated in the deposits outside the core. This activity transport accounts for the gradual rise in radiation fields around all out-core components in the HTS of all water-cooled nuclear power stations.

Each of these four observations will be discussed in detail with the emphasis on how coolant pH can reduce their importance to plant aging.

2. OUTLET FEEDER WALLING THINNING

The feeder pipes of existing CANDU reactors which convey heavy water into and away from the core are fabricated from carbon steel with a low chromium content. Periodic wall thickness measurements of these feeders were, until recently, performed on selected feeders at positions close to headers, and the results indicated that the metal loss from corrosion was acceptably small. However recent inspection of wall thickness in outlet feeder pipes close to the Grayloc fitting, connecting the fuel channel to the feeders, indicated wall loss rates were higher at the bends than near the headers.

The mechanism causing outlet feeder wall thinning was determined to be FAC from examination of a sample of outlet feeder pipe removed from a CANDU 6 reactor. The inside surface of the outlet feeder pipe sample at the first bend exhibited a regular pattern of intersecting polygonal depressions known as scallops, a morphology characteristic of surfaces that have experienced FAC.

Studies have shown that time, temperature, water chemistry, hydrodynamic and alloy composition variables affect the rate of FAC. The main water chemistry variables are pH and the degree of unsaturation in dissolved iron of the water relative to the solubility of magnetite. Under HTS conditions, the solubility of magnetite increases with increasing temperature and pH as shown in Figure 2. The coolant, after being heated in the core, emerges unsaturated in dissolved iron and dissolves the magnetite film on outlet feeder pipe surfaces. This is the reason for the wall loss being observed only on outlet feeder pipes, and not on inlet feeder pipes. The dissolved magnetite is subsequently precipitated on the surfaces of steam generator tubes and inlet feeder pipes and inlet end-fittings. Hence FAC modelling work (Burrill, 1995) suggested that operation towards the lower end of the operating pH range would result in lower rates of outlet feeder wall loss.

The results of jet impingement tests conducted at 310°C in a refreshed autoclave facility at CRL are plotted in Figure 3. They confirm that carbon steel corrosion rates increase with pH, within the range specified for CANDU. The results also confirm that the corrosion rate is proportional to the degree of unsaturation in dissolved iron. The data in this graph indicate a significant decrease in corrosion rate with a decrease in pH from $pH_a=10.8$ to $pH_a=10.2$. Based on an analysis of the results of the CRL short term tests, shifting the operating pH of CANDU reactors from levels near the upper end of the old specification ($10.2 \leq pH_a \leq 10.8$) to the current levels ($10.2 \leq pH_a \leq 10.4$) should result in 25-45% decreases in the corrosion rate.

To confirm the effect of lowering pH in an operating CANDU reactor, on-line ultrasonic (UT) wall thickness transducers have been installed on several outlet feeder pipes at two CANDU 6 plants to give on-line measurements of the rate of wall loss. Measurements are being made at both high and low pH values within the operating range. Preliminary results are still insufficient for conclusions regarding the effect of pH.

3. STEAM GENERATOR FOULING

A model describing the flow accelerated corrosion (FAC) of the carbon steel outlet feeders and the subsequent precipitation of magnetite on the tube bundle in the steam generator (SG) is described elsewhere (Burrill and Turner, 1994). The essential feature of the model is that the driving force for deposition is the difference between the concentration of dissolved iron in the primary coolant and the

solubility of magnetite at the surface of the SG tube. As the primary water is cooled, it becomes supersaturated in dissolved iron and deposition takes place. Steam generator fouling has two effects. First, the fouling deposits raise the heat transfer resistance across the tubes and generate an RIHT rise. Second, the fouling deposits increase the pressure drop along the tubes because of increased hydraulic roughness.

3.1 Reactor Inlet Header Temperature (RIHT) Rise

The iron deposition model described above has been incorporated into the THIRST thermohydraulics code to predict the effect of primary-side fouling on the increase in RIH temperature. Deposit profiles predicted by this model for a CANDU-6 SG after 10 EFPY are shown in Figure 4 for three different values of primary-coolant pH. These profiles show that the amount of magnetite predicted to precipitate onto the inside of the SG tubes is significantly reduced as the pH is reduced from 10.6 to 10.0.

The deposits that form on the inner surface of the tube bundle increase the resistance to heat transfer. This additional resistance to heat transfer is manifested by a rise in primary coolant temperature. Heat transfer through the primary-side deposit is by conduction through the magnetite crystals and through the stagnant water that fills the pores. The resulting conductivity of the deposit is a complex function of the porosity and of the conductivities of both water and magnetite (Turner et al. 1997).

Combining the results of the heat-transfer measurements with the calculated deposit loading allows one to predict the effect of a change in primary coolant pH on its contribution to the rise in RIH temperature. The results are shown in Figure 5 for different pH values. As expected, the contribution from primary-side deposition to the rise in RIHT decreases with decreasing pH. At the high-end of the pH range, primary-side fouling reaches the design fouling allowance within a period of 6 EFPY. Primary-side fouling is still a significant contributor to RIHT rise at pH 10.3, whereas at pH 10.0 its contribution is negligible for the lifetime of the plant.

Recent measurements of the thermal resistance of primary-side deposits have revealed an additional aging phenomenon not yet accounted for, namely that deposits may tend to become more conductive as a function of deposit thickness (Klimas et al., 1998). Evidence to date suggests that the average conductivity of the deposits could increase by as much as a factor of two. This would tend to flatten the curves in Figure 5 somewhat with increasing EFPY.

3.2 Increased Surface Roughness

Over time, the expectation was that the mass flow rate of coolant through the core would increase, and the header-to-header pressure drop would decrease due to diametral creep of pressure tubes. However, detailed analyses using the NUCIRC thermalhydraulics code indicate that while the header-to-header pressure drop has remained constant, the mass flow rate through the core has been slowly decreasing. This suggests that the surface roughness of the inlet and outlet piping and of the steam generator tube surfaces has been increasing.

A sensitivity analysis using NUCIRC indicated that the roughness of steam generator surfaces would account for a 2% reduction in core flow. A 2% reduction in core flow was also attributed to the roughness of the inlet feeders, while the roughness on the outlet feeders accounted for a 1% reduction in core flow.

The potential benefits of mechanical and chemical decontamination of steam generators on recovery of flow and heat transfer have been assessed in laboratory programs. Figure 6 shows the effect of chemical

cleaning and Figure 7 shows the effect of mechanical cleaning. The roughness is decreased from 300 to 400% greater than new tubes to 10 to 30%, based on comparisons to archived steam generator tubes. Therefore, the removal of deposits is expected to return the steam generator tubes to essentially their original surface roughness value.

4. FOULING OF INLET FEEDERS AND END-FITTINGS

Measurement of the surface roughness of inlet and outlet feeders before and after a full-HTS decontamination using CAN-DECON™ indicates that the roughness of inlet feeder pipes has been reduced. Thus, an almost complete flow recovery may be realized by removal of oxides from the inlet feeder pipes. Surface roughness measurements have been made on different portions of the HTS in different CANDU reactors. A summary of all surface roughness measurements is shown in Figure 8.

5. RADIATION FIELD GROWTH

The three established mechanisms for radionuclide generation are:

- activation of dissolved species and of particulates suspended in the coolant,
- activation of corrosion product particles deposited on the pressure tube and fuel sheath surfaces,
- irradiation of dissolved species adsorbed on these same surfaces.

A fourth mechanism suggested by current work is the activation of the growing magnetite deposit on the inlet bundle which is shuffled after one year to position 9 in the fuel channel. In its new position, the magnetite will dissolve quickly, but more radionuclides are created in the higher neutron flux while the magnetite dissolves. Figure 9 shows precipitated deposits on a fuel bundle from the inlet of a fuel channel at Bruce-6 NGS. Both the Bruce and Darlington stations refuel against the flow which means the inlet fuel bundle goes to the fuel bay and the fourth mechanism does not apply to them.

The iron transport theory was modeled to describe the FAC and precipitation processes at each location around the HTS. Then, models were added to predict the radionuclide release rate from the reactor core. Figure 10 shows the relative rates of Co-60 production for each of the two in-core processes and how they depend on coolant pH. There is less deposit on the inlet fuel bundles at low pH compared to high pH so there is less cobalt impurity to be irradiated in the deposit. The particulate mechanism depends on two factors that have opposing dependences on pH. First, particle concentrations in the coolant are lower, the lower the pH, which gives a lower deposition rate in the core. However, the lower pH gives a lower rate of particle dissolution. The net result is that the particulate mechanism is relatively insensitive to pH. Overall, the lower the pH, the lower the predicted radionuclide release rate and the lower the HTS radiation fields.

6. SUMMARY AND CONCLUSIONS

Both the available experimental evidence and the supporting 'iron transport' theory indicate that aging processes in CANDU plants can be reduced by operating the plants at lower pH. Reducing the coolant pH will lower the iron transport rate because of lower FAC on the outlet feeders. The less iron that is precipitating, the lower the fouling rate in the steam generator tubes and the lower the rate of RIHT rise. Data are examined for the surface roughness of corroded outlet feeder surfaces, but also for steam

generator and inlet feeder/inlet liner tube surfaces, but there is no evidence that thinner deposits will mean lower roughness.

7. ACKNOWLEDGEMENT

The authors gratefully acknowledge the pioneering effort of M. Soulard and G. Harvel at AECL Sheridan Park in developing and using the NUCIRC code to analyze HTS aging. We also are pleased to acknowledge H. Rummens for her work on pressure drop measurements on steam generator tubes and Y. Lu for his impinging jet work to establish the pH effect on flow accelerated corrosion.

8. REFERENCES

Burrill, K.A., and C.W. Turner, "Control of Reactor Inlet Header Temperature (RIHT) Rise in CANDU", CNA/COG Second International Steam Generator and Heat Exchanger Conference, Toronto, Ontario, 1994 June, AECL-11131/COG-94-386.

Burrill, K.A., "Modeling Flow Accelerated Corrosion in CANDU", Atomic Energy of Canada Limited report AECL-11397 (1995).

Burrill, K.A., "An Activity Transport Model for CANDU Based on Iron Transport in the Primary Coolant", Atomic Energy of Canada Limited report AECL-11805 (1998).

Klimas, S.J., D. Miller, J. Semmler, and C.W. Turner, "The Effect of the Removal of Steam Generator Tube Deposits on Heat Transfer". 3rd International Steam Generator and Heat Exchanger Conference, June 21-24, 1998, Toronto, Canada.

Sweeton, F.H., And Baes, Jr., C.F., 1970, "The Solubility of Magnetite and Hydrolysis of Ferrous Iron in Aqueous Solutions at Elevated Temperatures", *J. Chem. Thermodyn.*, 2 479-500.

Turner, C.W., and S.J. Klimas, "Thermal Resistance of Steam Generator Tube Deposits under Single-Phase Forced Convection and Flow Boiling Heat Transfer", COG-97-485-I/AECL-11887, October (1997).

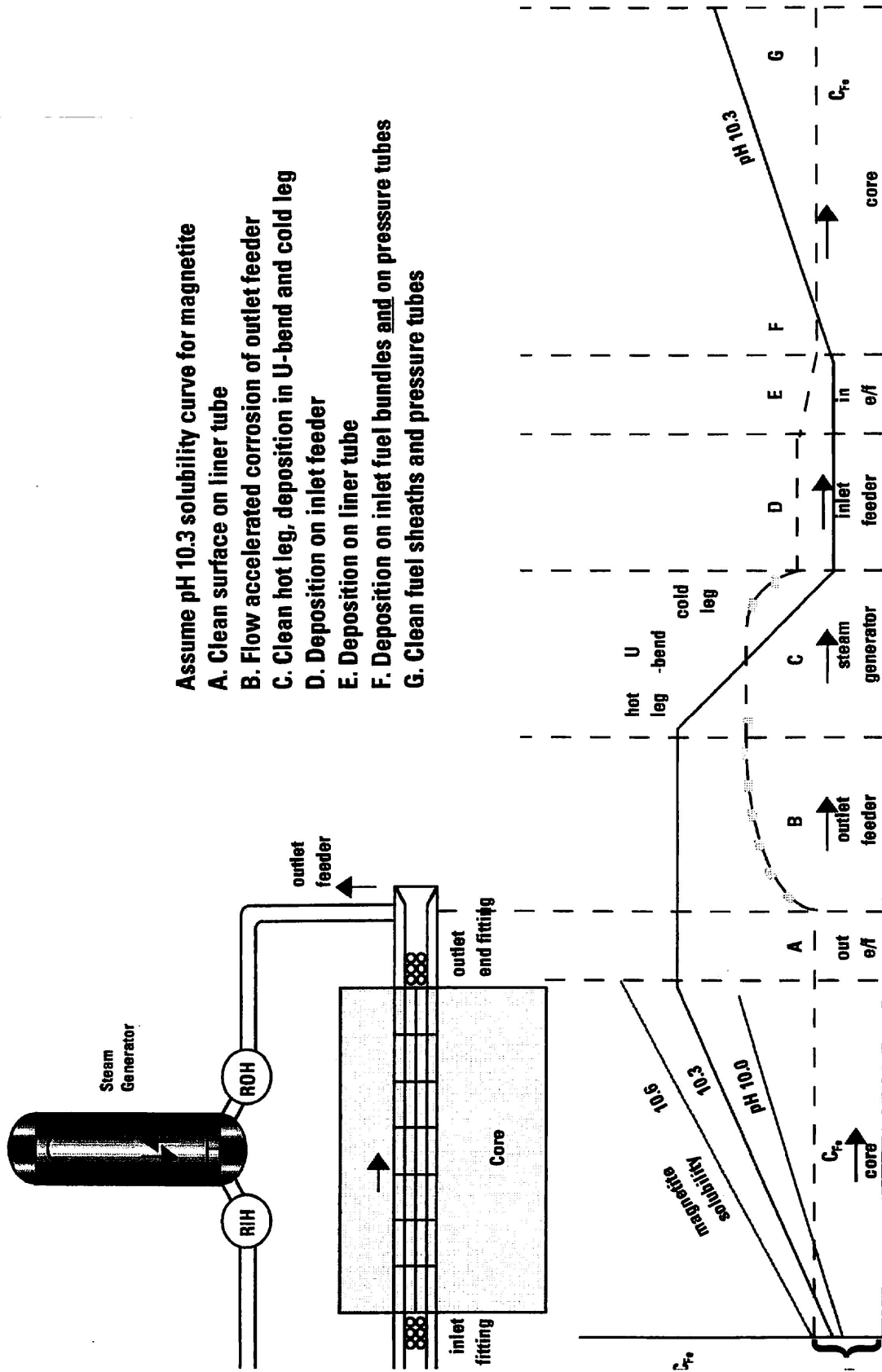


Figure 1 Profile of Dissolved Iron Concentration around CANDU Primary Circuit.

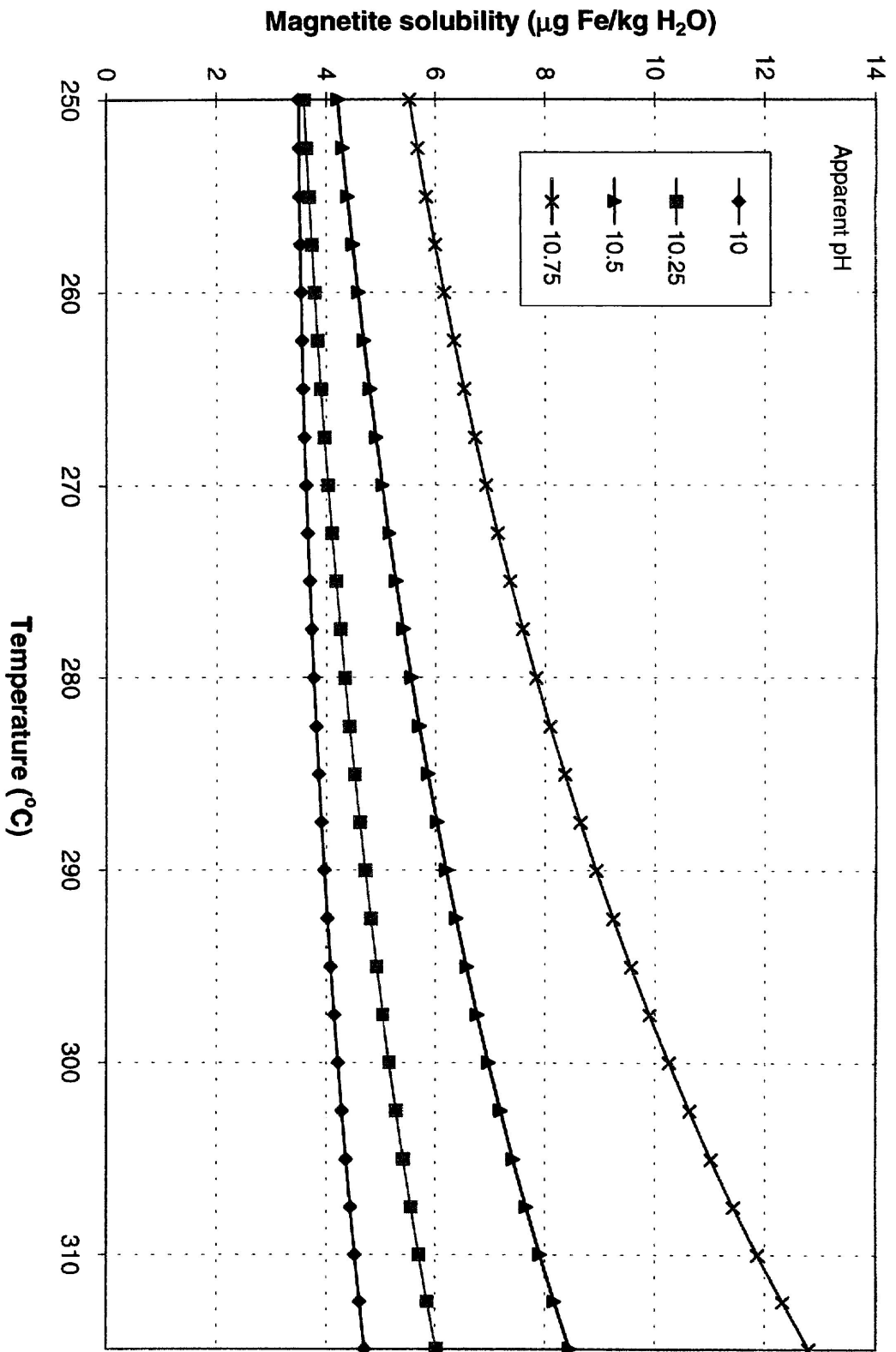
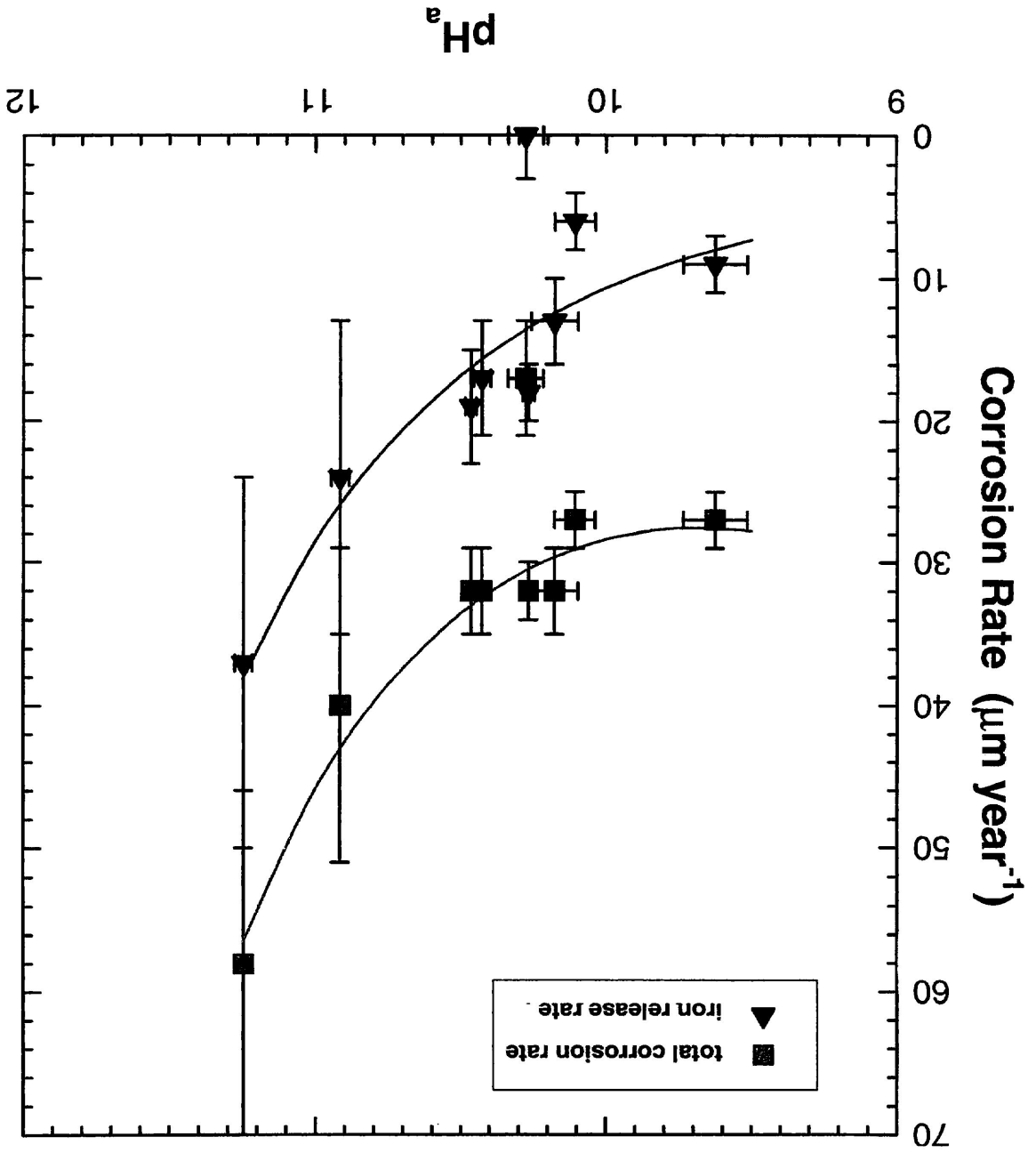


Figure 2 Effect of pH and Temperature on the Solubility of Magnetite According to Sweeton and Baes (1970).

Figure 3 Effect of pH_a on the Corrosion Rate of Type A106B Carbon Steel by Impinging Jet.



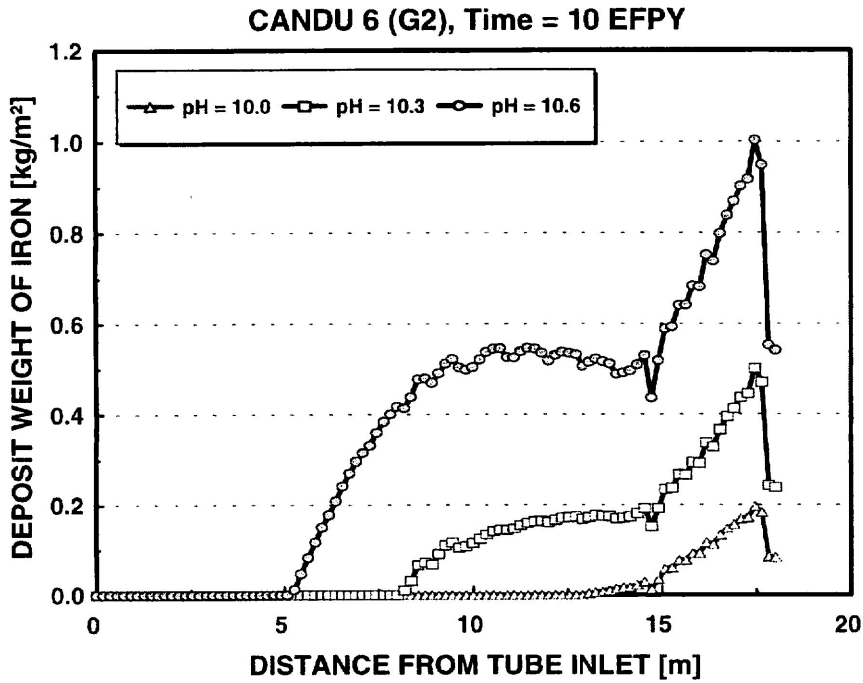


Figure 4 Effect of Primary Coolant pH on the Predicted Deposit Profile on the SG Tube Bundle.

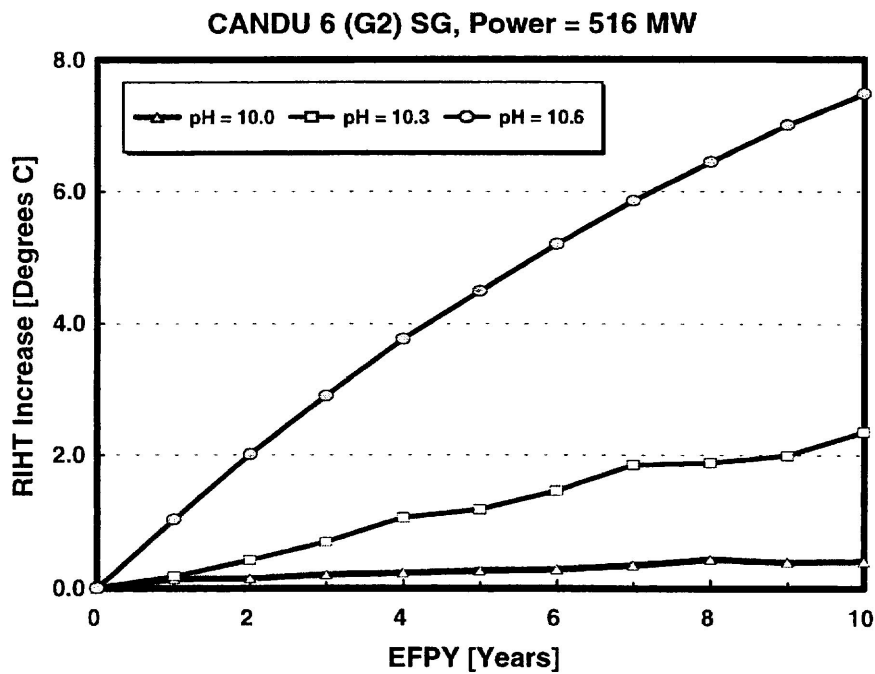


Figure 5 Effect of Primary Coolant pH on the Predicted Rise in RIHT from Primary Side Fouling.

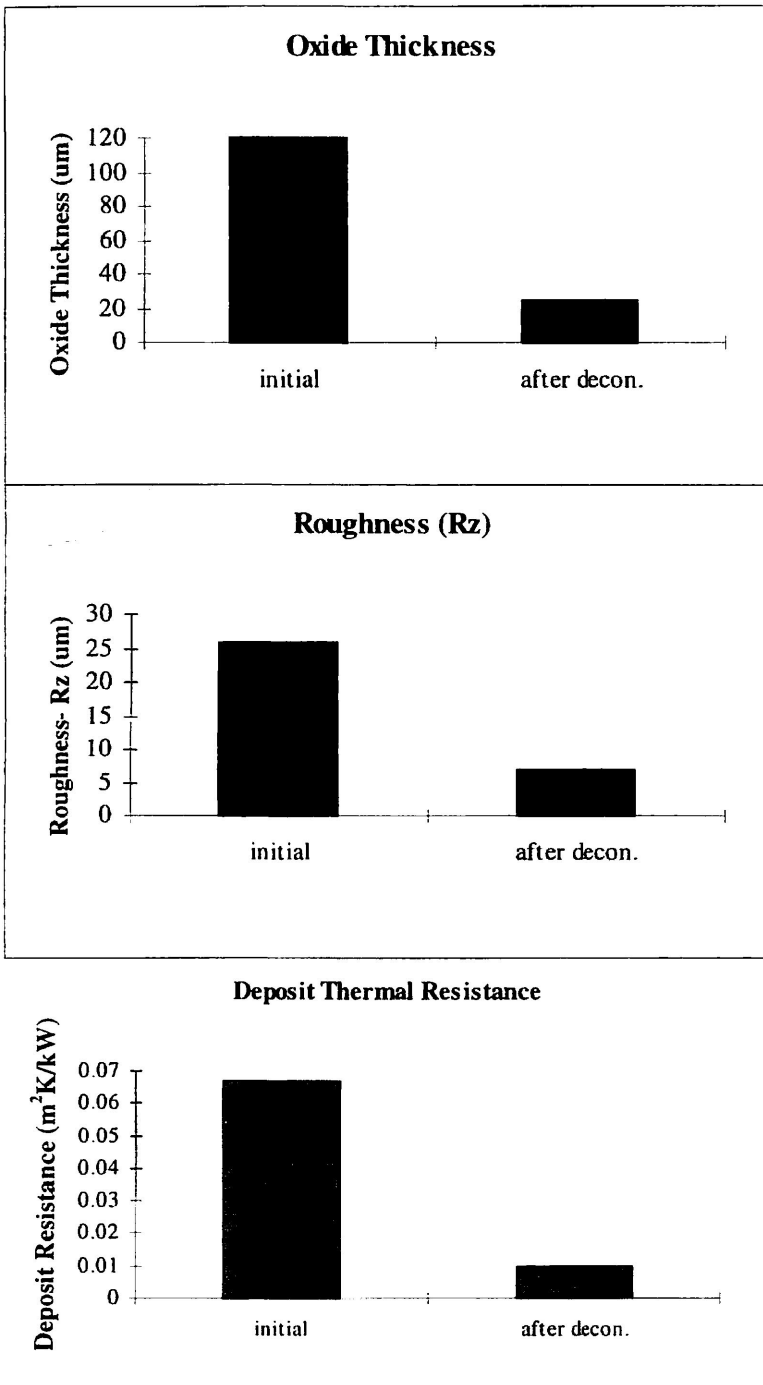


Figure 6 Oxide Loading, Surface Roughness, and Deposit Thermal Resistance after Chemical Decontamination of tubes from the Preheater Region of Gentilly-2 SG.

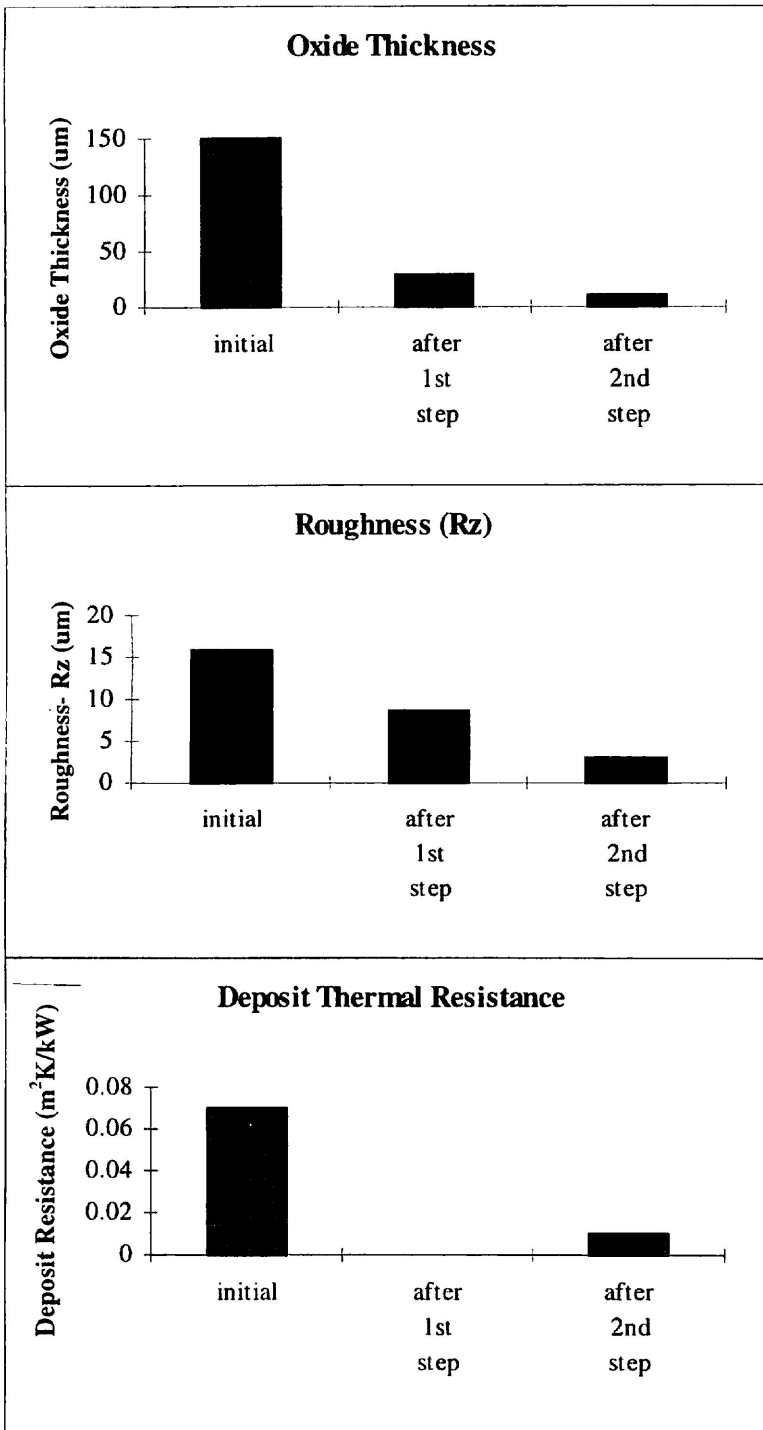


Figure 7 Oxide Loading, Surface Roughness, and Deposit Thermal Resistance after Mechanical Decontamination of tubes from the Preheater Region of Gentilly-2 SG.

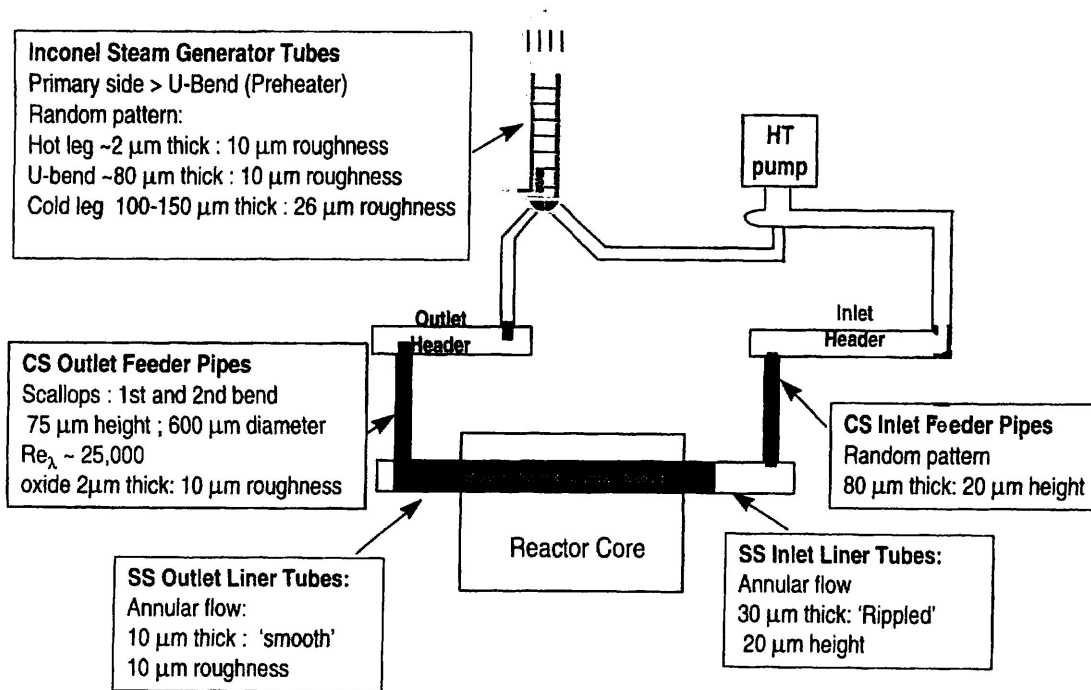
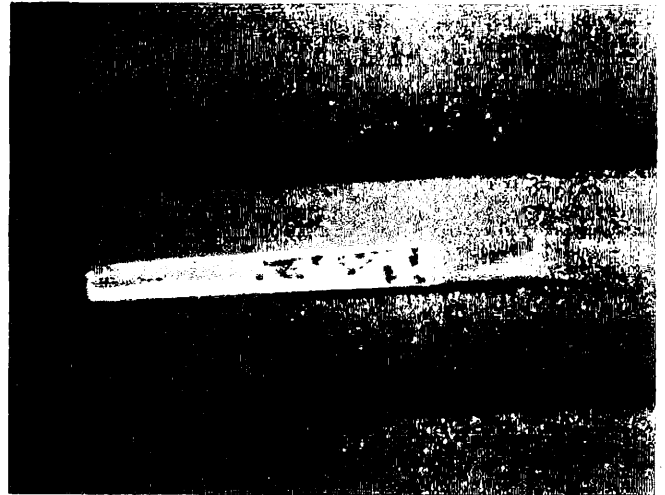


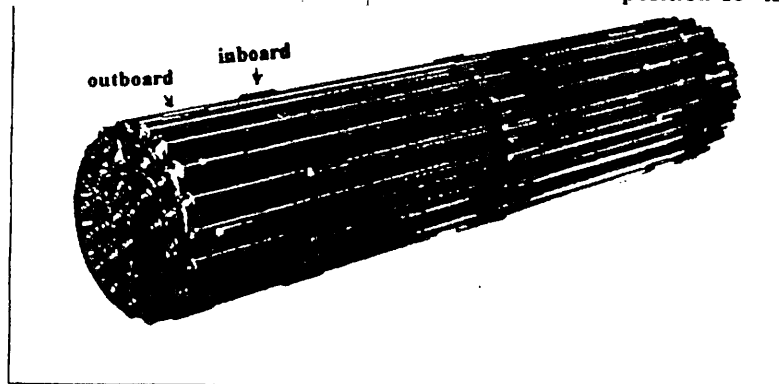
Figure 8 Summary of Surface Roughness Measurements around the HTS.



Bruce-6 X06 position 13 outboard 1986 April



Bruce-6 X06 position 13 inboard 1986 April



Bruce 37-Element Bundle



Bruce-6 M07. position 13 1986 April

Figure 9 Photographs of Deposits on Inlet Fuel Bundle at Bruce-B NGS.

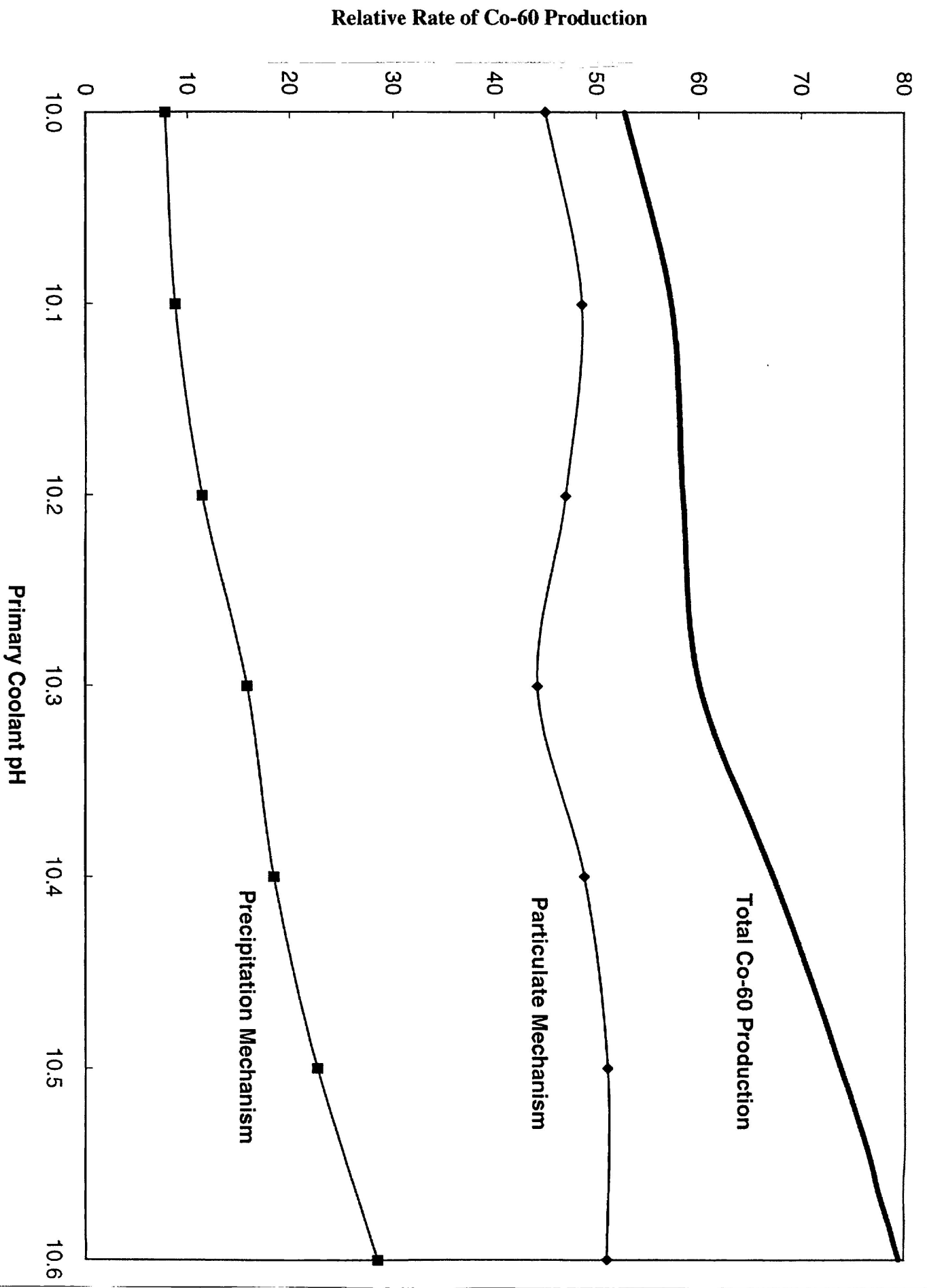


Figure 10 Effect of Primary Coolant pH on Co-60 Production Rate (after 5 EFPY) at Pickering-A NGS.